Supporting Information

'Donor-Acceptor', 'interpenetrating polymer network' and 'electrostatic self-assembly' work in tandem to achieve extraordinary specific shielding effectiveness

Amit Malakar, Samir Mondal, Ria Sen Gupta, Vinod Kashyap, Rishi Raj, Kunal Manna and Suryasarathi Bose[†], *

[†]Department of Materials Engineering, Indian Institute of Science, Bengaluru – 560012, India.

E-mail: * Corresponding Author Email address (sbose@iisc.ac.in)

Characterization techniques for the host-guest construct:

Morphological studies and elemental analyses were carried out with the use of an Ultra55 FE-SEM Karl Zeiss scanning electron microscope with an EDX detector and a transmission electron microscope (TEM, FEIG2 (Technai). TA Q500 was used for thermogravimetric analysis where the heating range was 35 ˚C to 800 ˚C at the heating rate of 10 ˚C/min. PANalytical X-Pert PRO apparatus with Cu K radiation (=1.54 A°) was used for XRD (X-ray Diffraction) analysis. The density of the ACNT/PDDA powder was determined using a Quantachrome India Helium gas Pycnometer (Model No.- ULTRAPYC 1200e). Raman analysis was carried out utilizing LabRAM HR and a CCD detector. The Zeta-potentials of the guest solution mixture particles and host membrane were measured using a Zeta-potential analyzer (Malvern Instruments' Zetasizer Nano ZS90) and an electro-kinetic analyzer (Anton Par's SurPASS) respectively. The electrical conductivities of all four constructs were measured at room temperature on evenly polished and compression-molded discs with a thickness of 1 mm using an Alpha-N analyzer from Novocontrol (Germany) with Vrms at 1 V throughout a wide frequency range of 0.1 Hz to 10 MHz. Surface conductivities at room temperature were measured with a four-probe approach in a Keithley 2420-C source meter. Polytec MSA-500 Micro-system analyzer was used for optical profilometry. . Using an Agilent vector network analyzer (VNA) in the X band (frequency range = 8.2 to 12.4 GHz), the EMI shielding qualities of all the constructs were assessed. The Vidyut Yantra Udyog (KU7061; S.N. 2454) waveguide was connected to the VNA.

FTIR analysis was carried out to evaluate the chemical surroundings of the m-IPN membranes (Fig. 1a). A novel peak at 1715 cm^{-1} could be attributed to the -C=O imide bond in BMI [1/23] in addition to the typical absorption peak that typically results from PVDF/PDA IPN membranes.[2/18] Additionally, the good integration of BMI is shown by the purposeful absence of the N-H bending peak at 1635 cm^{-1} in m-IPN. The increase in C=C bonds caused by the presence of GO may be the cause of the increase in the absorption peak intensity.

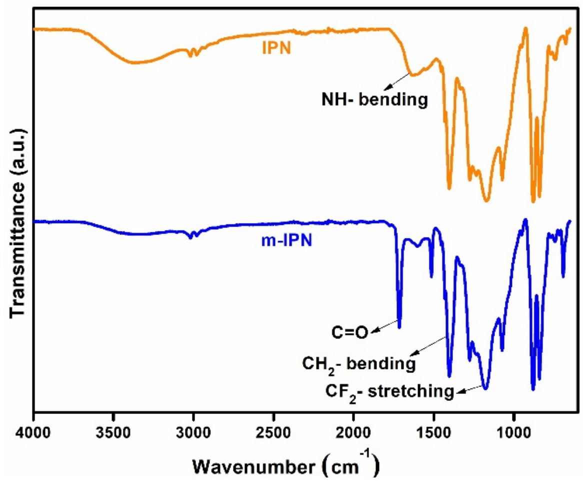

Fig. S1: FTIR plot for IPN and m-IPN (I)

Theory of Electromagnetic Interference (EMI) Shielding

The capacity of a material to reduce the energy of incident electromagnetic waves is known as EMI SE. The shielding phenomena is controlled by the contributions from reflection (SE_R), absorption (SE_A), and multiple internal reflections (SE_M) when the electromagnetic radiations interact with the material under test (shield). The sum of the contributions from SE_R, SE_A, and SE_M is known as the total EMI SE (SET). The total SE_T can be written as ;

$$SE_T = SE_A + SE_R + SE_M \qquad \text{(S1)}$$

When SE_T is greater than 15 dB, SE_M is typically regarded as inconsequential for computations. The scattering parameters S_{11} (forward reflection coefficient), S_{12} (forward transmission coefficient), S_{21} (backward transmission coefficient), and S_{22} (reverse reflection coefficient) are used in vector network analyzers to represent EMI SE. These equations[3] can be used to calculate the SE_T from the S parameters.)

$$SE_R = 10 \log\left(\frac{1}{1-R}\right) = 10 \log \frac{1}{1-|S_{11}|^2} \qquad \text{(S2)}$$

$$SE_A = 10\log\left(\frac{1-R}{T}\right) = 10\log\frac{1-|S_{11}|^2}{|S_{21}|^2} \quad (S3)$$

Equation (S1) can be used to calculate the Fresnel formula (S4) for reflection, absorption, and multiple reflections under the assumption that electromagnetic waves propagate through a nonmagnetic, highly conducting material.

$$SE_T = 10\log\left(\frac{1}{T}\right) = 10\log\left(\frac{1}{|S21|^2}\right) = 10\log\left(\frac{Ei}{Et}\right) = 20\log\left|\frac{(1+N)^2}{4N}e^{-kd}\left[1-\left(\frac{1-N}{1+N}\right)^2 e^{2ikT}\right]\right|$$

(S4)

where E_i and E_t are incident and transmitted intensities of electric field of the EM waves, respectively; N is the complex refractive index of the shield, k is the imaginary part of refractive index, and t is the shield thickness.

The EMI Shielding efficiency % can be calculated by the following equation.

$$Shielding\ Efficiency\,\% = 100 - \left(10^{\frac{SE}{10}}\right)^{-1} \times 100 \quad (S5)$$

Where, SE stands for total shielding efficiency i.e.

From equation S4, the quantitative estimation of SE_A can be obtained by following equation:

$$SE_A = 8.686\,\alpha t \quad (S6)$$

Where α represent the attenuation constant.

Further, Skin depth (δ), which explains the intensity of penetration, can be calculated by equation S7 :

$$SE_A = 8.686\,\frac{t}{\delta} \quad (S7)$$

Where, t stands for shield thickness.

The green index (gs) of shielding material is calculated using Eq. S8 as below:

$$g_s = \frac{1}{(S_{11})^2} - \frac{(S_{21})^2}{(S_{11})^2} - 1 \quad (S8)$$

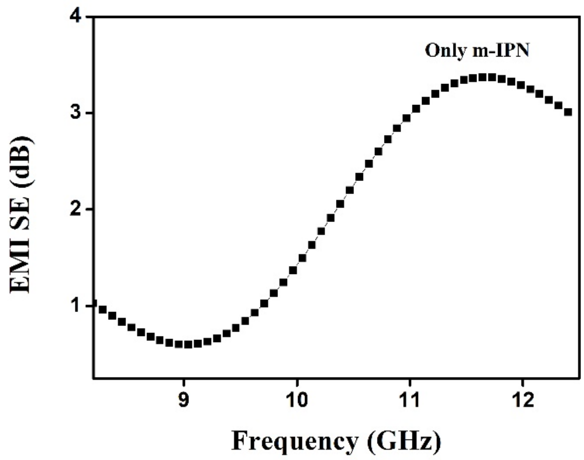

Fig. S2: Plot of EMI SE vs frequency in X-band for m- IPN (I).

References:

1. M, S. C.; Krishna, M.; Salini, K.; Rai, K. S. Preparation and Characterization of Chain-Extended Bismaleimide / Carbon Fibre Composites. **2010**, *2010*. https://doi.org/10.1155/2010/987357.
2. Gupta, R. Sen; Padmavathy, N.; Agarwal, P.; Bose, S. PH-Triggered Bio-Inspired Membranes Engineered Using Sequential Interpenetrating Polymeric Networks for Tunable Antibiotic and Dye Removal. *Chem. Eng. J.* **2022**, *446* (P2), 136997. https://doi.org/10.1016/j.cej.2022.136997.
3. Manna, K.; Gupta, R. Sen; Bose, S. A Universal Approach to 'Host' Carbon Nanotubes on a Charge Triggered 'Guest' Interpenetrating Polymer Network for Excellent 'Green' Electromagnetic Interference Shielding. **2023**, 1373–1391. https://doi.org/10.1039/d2nr05626g.